International Journal of Stem Cells Vol. 6, No. 2, 2013

ORIGINAL ARTICLE

Histological Experimental Study on the Effect of Stem Cell Therapy on Adriamycin Induced Chemobrain

Maha Baligh Zickri[1], Dalia Hussein Abd El Aziz[2], Hala Gabr Metwally[3]

Department of Histology, Faculty of Medicine, [1]Cairo University, [2]Beni-Suef University, [3]Department of Clinical Pathology, Faculty of Medicine, Cairo University, Cairo, Egypt

Background and Objectives: Negative consequences of chemotherapy on brain function were suggested and were addressed in animal models as the clinical phenomenon of chemobrain .It was postulated that adriamycin (ADR) induce changes in behaviour and in brain morphology. Human umbilical cord mesenchymal stem cells (HUCMSCs) could be induced to differentiate into neuron-like cells .The present study aimed at investigating the possible therapeutic effect of HUCMSC therapy on adriamycin induced chemobrain in rat.

Methods and Results: Twenty five female albino rats were divided into control group, ADR group where rats were given single intraperitoneal (IP) injection of 5 mg/kg ADR. The rats were sacrificed two and four weeks following confirmation of brain damage. In stem cell therapy group, rats were injected with HUCMSCs following confirmation of brain damage and sacrificed two and four weeks after therapy. Brain sections were exposed to histological, histochemical, immunohistochemical and morphometric studies. In ADR group, multiple shrunken neurons exhibiting dark nuclei and surrounded by vacuoles were seen .In response to SC therapy ,multiple normal pyramidal nerve cells were noted. The area of shrunken nerve cells exhibiting dark nuclei, Prussion blue and CD105 positive cells were significantly different in ADR group in comparison to SC therapy group.

Conclusions: ADR induced progressive duration dependant cerebral degenerative changes. These changes were ameliorated following cord blood human mesenchymal stem cell therapy. A reciprocal relation was recorded between the extent of regeneration and the existence of undifferentiated mesenchymal stem cells.

Keywords: Mesenchymal stem cells, Adriamycin, Cord blood, Chemobrain

Introduction

Chemotherapy drug combinations were proved to induce effect on various aspects of learning and memory. Chemotherapy-associated cognitive dysfunction was postulated. Spatial learning, memory ability as well as discrimination learning were tested in rats receiving chemotherapy combinations. Negative consequences of chemotherapy on brain function were suggested and were addressed in animal models as the clinical phenomenon of chemobrain (1).

Breast cancer is the most common malignancy among women, and considered a leading cause of cancer deaths. Doxorubicin (adriamycin) has been developed for the treatment of metastatic breast cancer (2). Administration of chemotherapy during the fetal phase of pregnancy may put late-developing organs like the central nervous system at risk. The current preclinical data reveal changes in behaviour and transiently also in brain morphology in the mice that were prenatally exposed to doxorubicin (3).

The mesenchymal stem cells (MCSs) derived from umbilical cord tissue have low immunogenicity and contain few immune cells. Previously, studies demonstrated that

Accepted for publication August 31, 2013
Correspondence to **Maha Baligh Zickri**
Department of Histology, Faculty of Medicine, Cairo University, Cairo, Egypt
Tel: +20123955078, Fax: +20235381183/+20235381760
E-mail: mahakaah@yahoo.com

human umbilical cord MSCs could be induced to differentiate into neuron-like cells (4).

The present study aimed at investigating the possible therapeutic effect of human cord blood mesenchymal stem cell therapy on adriamycin induced chemobrain in albino rat.

Material and Methods

Twenty five female albino rats weighing 150～200 g were used and divided into 3 groups placed in separate cages. The animals were kept under good hygienic conditions, fed ad libitum and allowed for free water supply. The experiment was performed in the Animal House of Histology Department, Faculty of Medicine, Cairo University. The rats were treated in accordance with guidelines approved by the Animal Use Committee of Cairo University. The rats were divided into groups and subgroups:

Control group: 4 rats, one for each of the corresponding experimental subgroups. Each animal received single intraperitoneal (IP) injection of 0.5 ml distilled water.

Group A (Adriamycin group): 11 rats each received 5 mg/kg (5) of adriamycin (ADR) (Pharmacia Italia Corporation), using 10 mg vials. ADR was administered by IP injection (6) at a single dose (7) dissolved in 0.5 ml distilled water. One rat was sacrificed thirty days following the day of injection for confirmation of brain damage. The remaining rats were subdivided into:

Subgroup (A1): Five animals were sacrificed 2 weeks following the confirmation of brain damage.

Subgroup (A2): Five animals were sacrificed 4 weeks following the confirmation of brain damage.

Group S (Stem cell (SC) therapy group): 10 rats received ADR by the same route, at the same frequency of administration and at the same dose as in the previous group. They were injected with 0.5 ml of cultured and labeled human mesenchymal stem cells (HMSCs) suspended in phosphate buffer saline (PBS) in the tail vein (8). The injection was performed on two successive days following confirmation of cerebral damage. Stem cells were isolated from cord blood (9). Cord blood collection was performed at the Gynaecology Department, Faculty of Medicine, Cairo University. Stem cell isolation, culture, labeling and phenotyping were performed at Hematology Unit, New Kasr El Aini Teaching Hospital. The rats were subdivided into:

Subgroup (S1): Five rats sacrificed 2 weeks following Sc therapy.

Subgroup (S2): Five rats sacrificed 4 weeks following Sc therapy.

Cord blood collection (10)

The storage and transport temperature was 15～22°C, transport time was 8～24 hours, sample volume was 65～250 ml. No sample had signs of coagulation or hemolysis.

Mononuclear cell fraction isolation (10)

The mononuclear cell fraction (MNCF) was isolated by carefully loading 30 ml of whole blood onto 10 ml of Ficoll density media (Healthcare Bio-Sciences) in 50 ml polypropylene tubes. Centrifuge for 30 minutes at room temperature at 450×g and the interphase collected after aspirating and discarding the supernatant. The interphase was washed with 20 ml PBS and centrifuged at 150×g for 5 minutes at room temperature. The supernatant was aspirated and the cells were washed with PBS a second time. The cells were re-suspended in the isolation media to prevent adherence of monocytic cells. The isolation media was low-glucose DMEM (Dulbecco's modified Eagles medium) (Cambrex Bio Science, Minnesota, USA), penicillin (100 IU/ml) (Invitrogen), streptomycin (0.1 mg/ml) and ultraglutamine (2 mM) (Cambrex Bio-Science). Incubation was at 38.5°C in humidified atmosphere containing 5% CO_2.

Culture (10)

The isolation media were replaced after overnight incubation (12～18 hours) in order to remove non-adherent cells. The media were replaced every 3 days until MSC colonies were noted. The cultures were inspected daily for formation of adherent spindle-shaped fibroblastoid cell colonies. Sub-culturing was done by chemical detachment using 0.04% trypsin. Later, when cell numbers allowed expansion was done in 25 cm^2 or 75 cm^2 tissue culture flasks.

Labeling (11)

Mesenchymal stem cells were labeled by incubation with ferumoxides injectable solution (25 microgramFe/ml, Feridex, Berlex Laboratories) in culture medium for 24 hours with 375 nanogram/ml poly L lysine added 1 hour before cell incubation. Labeling was histologically assessed using Prussian blue. Feridex labeled MSCs were washed in PBS, trypsinized, washed and resuspended in 0.01 Mol/L PBS at concentration of 1×1,000,000 cells/ml.

Cell viability analysis

Cell viability was done using trypan blue dye exclusion test. This method is based on the principle that viable cells do not take up certain dyes, whereas dead cells do.

Flow cytometry (12)

Flow cytometric analyses were performed on a Fluore-

scence Activated Cell Sorter (FACS) flow cytometer (Coulter Epics Elite, Miami, FL, USA). HMSC were trypsinized and washed twice with PBS. A total number of 1×100000 HMSC were used for each run. To evaluate the HMSC marker profile, cells were incubated in 100 μl of PBS with 3 μl of CD105-FITC for 20 min at room temperature. Antibody concentration was 0.1 mg ml^{-1}. Cells were washed twice with PBS and finally diluted in 200 μl of PBS. The expression of surface marker was assessed by the mean fluorescence. CD105 (mesenchymal stem cell marker), CD133 (early hematopoietic & endothelial progenitor stem cell marker) and CD45 (panleucocytic marker) were also used. The percentage of cells positive for CD105 was determined by subtracting the percentage of cells stained non-specifically with isotype control antibodies.

The rats were sacrificed using lethal dose of ether. The skull was broken using bone cutter, brain specimens were obtained, fixed in 10% formol saline for 48 hours, paraffin blocks were prepared and 5 μm thick sections were subjected to the following studies.

Histological study

Hematoxylin and eosin (H&E) stain (13).

Histochemical study

Prussian blue (Pb) stain (14) for demonstration of iron oxide labeled therapeutic stem cells.

Immunohistochemical study

CD105 immunostaining (15) the marker for HMSCs. 0.1 ml prediluted primary antibody CD105 rabbit polyclonal Ab (ab27422) and incubate at room temperature in moist chamber for 30～60 minutes. Tonsil used as positive control specimens. Cellular localization is the cell membrane. On the other hand, one of the brain sections was used as a negative control by passing the step of applying the primary antibody.

Morphometric study

Using Leica Qwin 500 LTD (Leica LTD, Cambridge, UK) image analysis, assessment of the area of shrunken nerve cells wih dark nuclei using interactive measurements menu was done in 10 high power fields (HPF). The area% of Pb+ve cells and that of CD105+ve cells were estimated in 10 HPF using binary mode.

Statistical analysis (16)

Quantitative data were summarized as means and standard deviations and compared using one-way analysis-of variance (ANOVA). p-values <0.05 were considered statistically significant. Calculations were made on SPSS software.

Results

Hematoxylin and eosin (H&E) stained sections

Cerebral cortex sections of control rats demonstrated pyramidal neurons and neuropil inbetween (Fig. 1). Closer observation revealed the pyramidal neurons exhibiting basophilic cytoplasm and pale nuclei. Small dark nuclei of neuroglial cells were seen inbetween (Fig. 2).

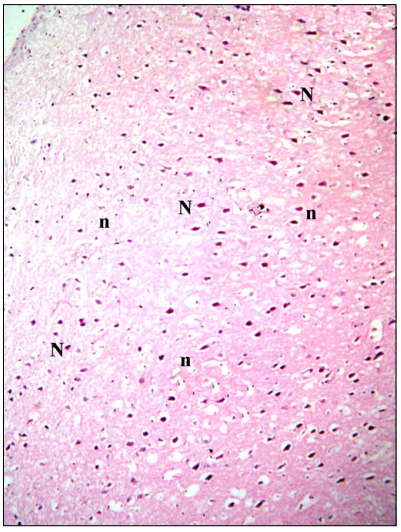

Fig. 1. Section in the cerebral cortex of a control rat showing pyramidal neurons (N) and neuropil (n) inbetween (H&E, ×100).

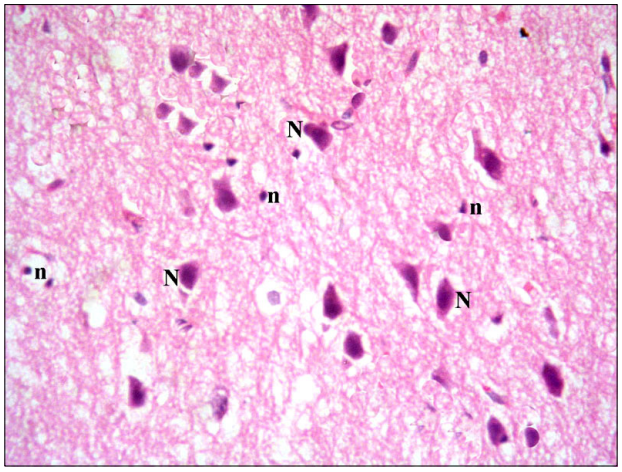

Fig. 2. Section in the cerebral cortex of a control rat showing pyramidal neurons (N) with basophilic cytoplasm and pale nuclei. Note small dark nuclei of neuroglial cells (n) (H&E, ×400).

In subgroup A1 (rats sacrificed two weeks following confirmation of brain damage), some fields showed multiple vacuoles in the superficial layer of the cerebral cortex. Some dark nuclei and occasional vacuoles containing cellular debris were seen in the deeper layers (Fig. 3). Some shrunken nerve cells exhibiting dark nuclei and surrounded by vacuoles existed in some fields by closer observation. Some normal pyramidal cells were also noticed (Fig. 4).

In subgroup A2 (rats sacrificed four weeks following confirmation of brain damage), partial separation of the surface of the cerebral cortex from the underlying layers was noticed. Large vacuoles were observed in the superficial layers. Multiple dark nuclei of the neurons and multiple vacuoles containing cellular debris were detected in the deeper layers (Fig. 5). Multiple shrunken neurons exhibiting dark nuclei and surrounded by vacuoles were seen by close observation (Fig. 6).

In subgroup S1 (rats sacrificed two weeks following SC therapy), some fields showed localized areas recruiting vacuoles and multiple dark nuclei. Occasional distended and occasional congested vessels were seen (Fig. 7). Closer ob-

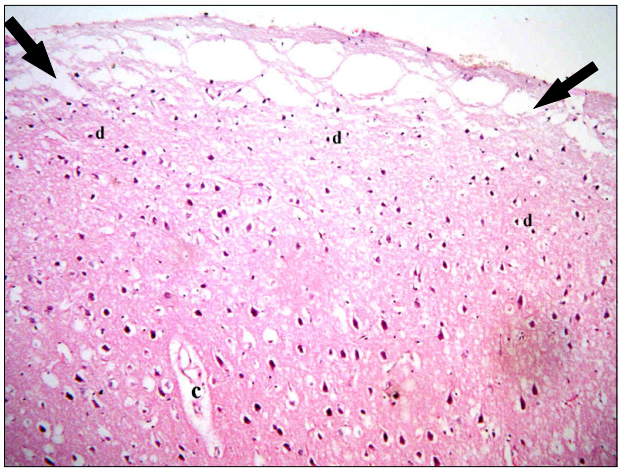

Fig. 3. Section in the cerebral cortex of a rat in subgroup A1 (rats sacrificed two weeks following confirmation of brain damage) showing multiple vacuoles (arrows) in the superficial layer of the cerebral cortex, some dark nuclei (d) of nerve cells and a vacuole containing cellular debris (c) (H&E, ×100).

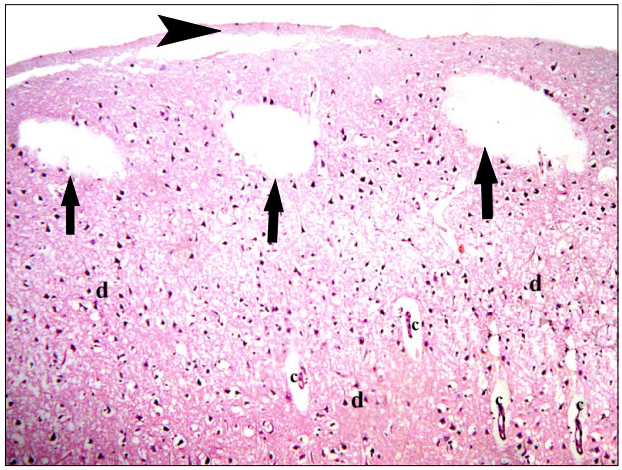

Fig. 5. Section in the cerebral cortex of a rat in subgroup A2 (rats sacrificed four weeks following confirmation of brain damage) showing separation of the surface (arrowhead), large vacuoles (arrows), multiple dark nuclei (d) of the neurons and multiple vacuoles containing cellular debris (c) (H&E, ×100).

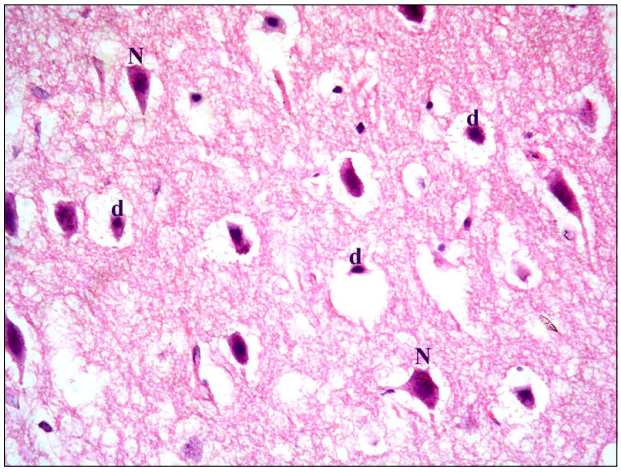

Fig. 4. Section in the cerebral cortex of a rat in subgroup A1 showing shrunken nerve cells with dark nuclei (d) and surrounded by vacuoles. Note some normal pyramidal cells (N) (H&E, ×400).

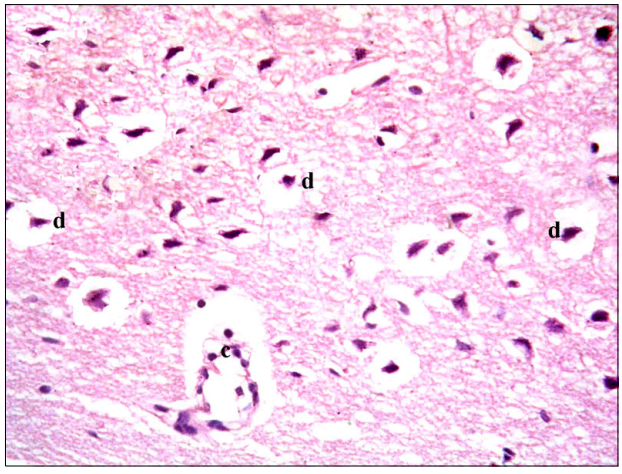

Fig. 6. Section in the cerebral cortex of a rat in subgroup A2 showing multiple shrunken neurons with dark nuclei (d) and surrounded by vacuoles. Note a vacuole containing cellular debris (c) (H&E, ×400).

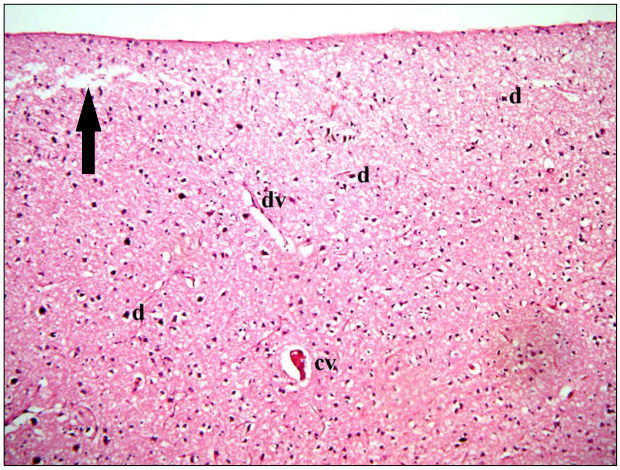

Fig. 7. Section in the cerebral cortex of a rat in subgroup S1 (rats sacrificed two weeks following SC therapy) showing a localized area of vacuoles (arrow), multiple dark nuclei (d), a distended vessel (dv) and a congested vessel (cv) (H&E, ×100).

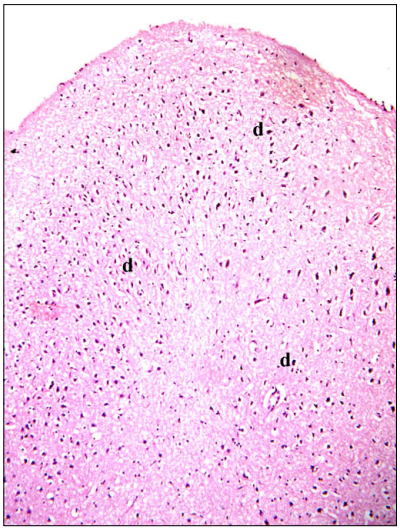

Fig. 9. Section in the cerebral cortex of a rat in subgroup S2 (rats sacrificed four weeks following stem cell therapy) showing some nerve cells with dark nuclei (d) (H&E, ×100).

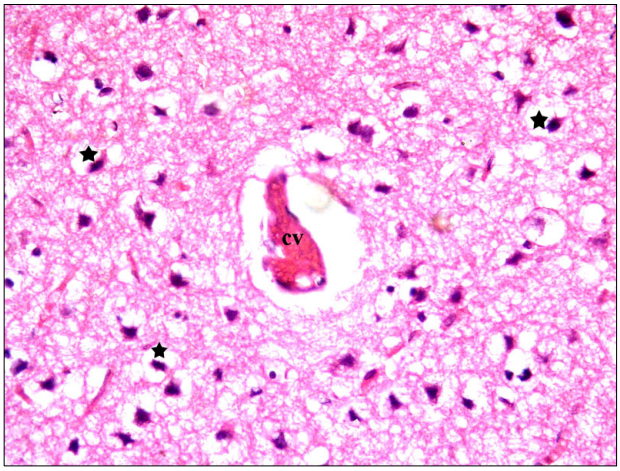

Fig. 8. Section in the cerebral cortex of a rat in subgroup S1 showing some shrunken nerve cells with dark nuclei and surrounded by minimal vacuoles (*). Note the congested vessel (H&E, ×400).

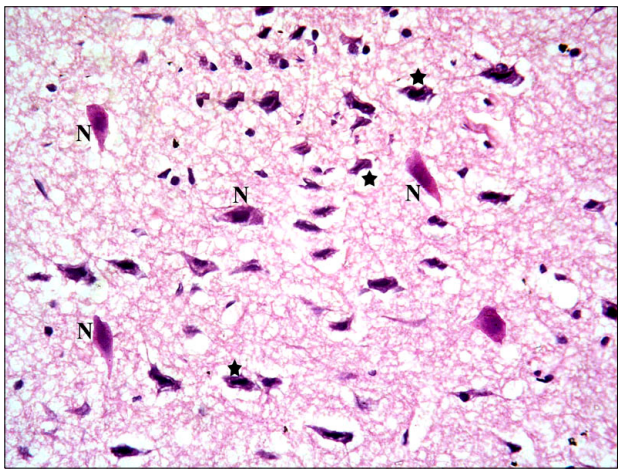

Fig. 10. Sections in the cerebral cortex of a rat in subgroup S2 showing some shrunken nerve cells with dark nuclei and surrounded by minimal vacuoles (*). Note multiple normal pyramidal nerve cells (N) (H&E, ×400).

servation revealed some shrunken nerve cells containing dark nuclei and surrounded by minimal vacuoles (Fig. 8).

In subgroup S2 (rats sacrificed four weeks following SC therapy), some nerve cells with dark nuclei were found (Fig. 9). Closer observations showed some shrunken nerve cells with dark nuclei and surrounded by minimal vacuoles. Multiple normal pyramidal nerve cells were also noted (Fig. 10).

Prussian blue stained sections

Sections in the cerebral cortex of control rats showed negative staining with Pb (Fig. 11). In SC therapy subgroup S1, some fields showed multiple spindle and few cuboidal positive (+ve) cells inside and near blood vessels (Figs. 12, 13). In addition, subgroup S2 showed few spindle and cuboidal +ve cells (Fig. 14) in some fields and occasional cuboidal +ve cells in some others among the neurons (Fig. 15).

CD105 immunostained sections

Sections in the cerebral cortex of control rats showed negative immunostaining with CD105 (Fig. 16). The SC therapy subgroup S1 showed multiple spindle, branched and cuboidal CD105 +ve cells. Some of the +ve cells ap-

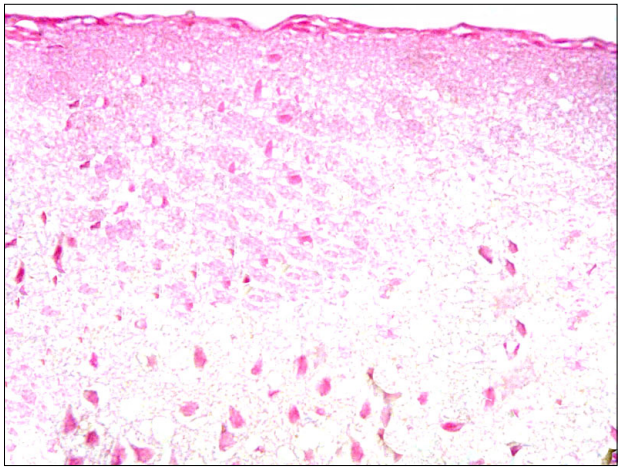

Fig. 11. Section in the cerebral cortex of a control rat showing negative reaction (Prussian blue, ×400).

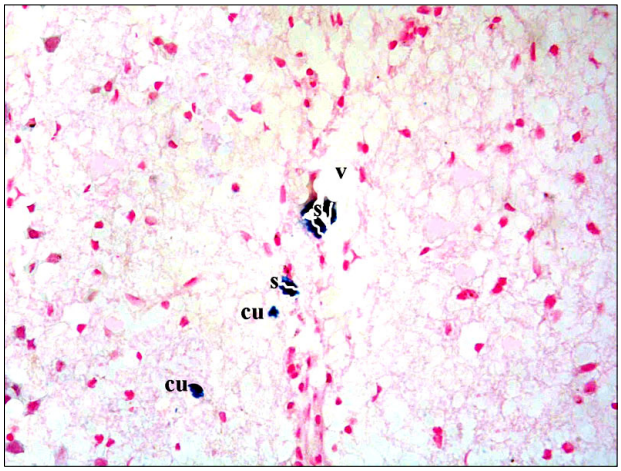

Fig. 12. Section in the cerebral cortex of a rat in subgroup S1 showing multiple spindle (s) and few cuboidal (cu) PB+ve cells inside and near a blood vessel (v) (Prussian blue, ×400).

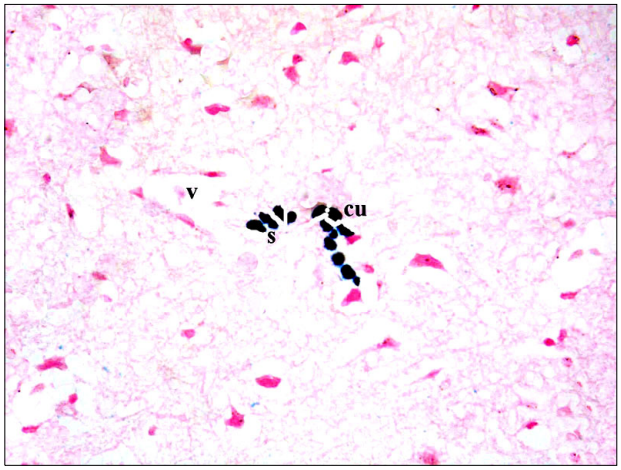

Fig. 13. A rat in subgroup S1 showing multiple spindle (s) and cuboidal (cu) Pb+ve cells near a blood vessel (v) (Prussian blue, ×400).

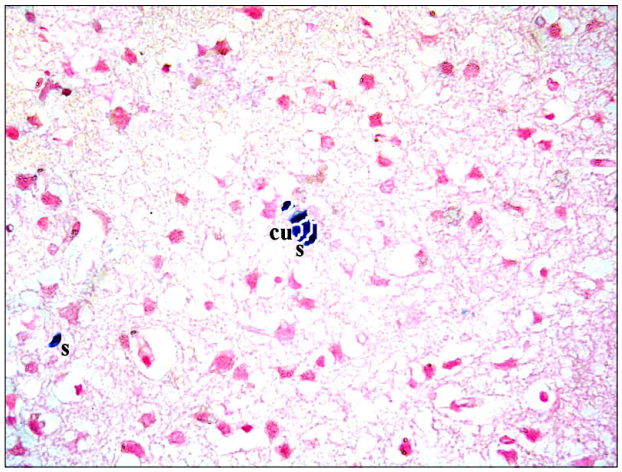

Fig. 14. A rat in subgroup S2 showing some spindle (s) and a cuboidal (cu) Pb +ve cells among the neurons (Prussian blue, ×400).

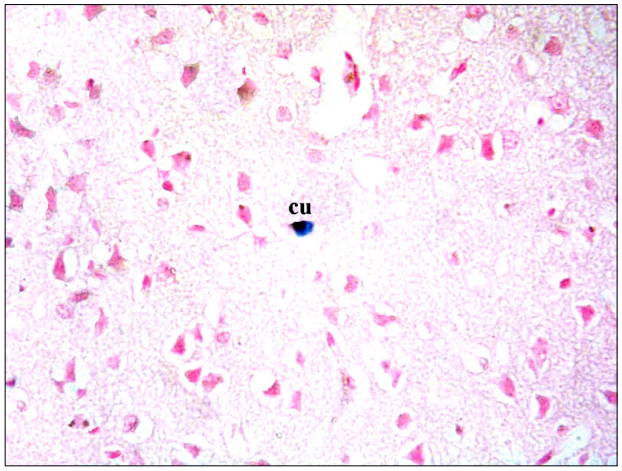

Fig. 15. A rat in subgroup S2 showing a cuboidal (cu) Pb+ve cell among the neurons (Prussian blue, ×400).

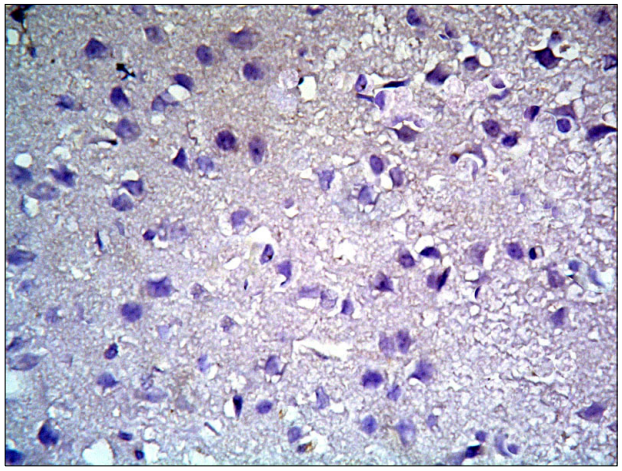

Fig. 16. Section in the cerebral cortex of a control rat showing negative immunostaining (CD105 immunostaining x400).

peared inside blood vessels and others were seen near blood vessels (Fig. 17). On the other hand, subgroup S2 showed few spindle, branched and cuboidal +ve cells near blood vessels (Fig. 18).

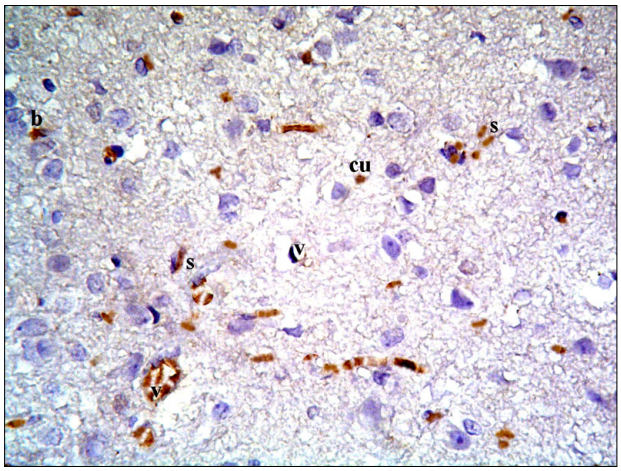

Fig. 17. Section in the cerebral cortex of a rat in subgroup S1 showing multiple spindle (s), cuboidal (cu) and branched CD105 +ve cells inside and near blood vessels (v) (CD105 immunostaining ×400).

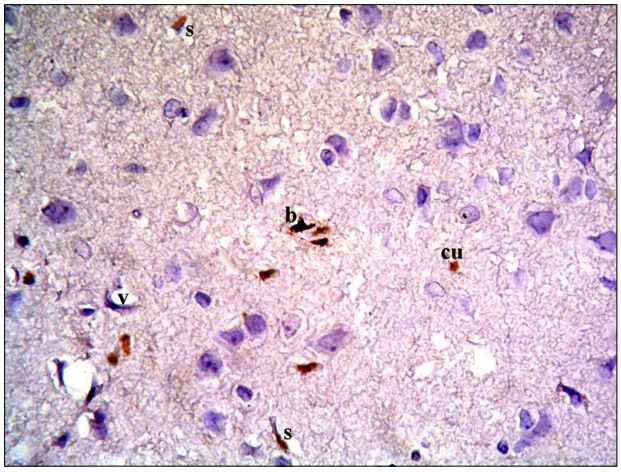

Fig. 18. Section in the cerebral cortex of a rat in subgroup S2 showing few spindle (s), cuboidal (cu) and branched (b) CD105 +ve cells near blood vessels (v) (CD105 immunostaining ×400).

Morphometric results

The area of shrunken nerve cells exhibiting dark nuclei recorded a significant ($p<0.05$) increase in subgroup A2 compared to subgroups A1, S1 and S2 (Table 1). On the other hand, the area% of Pb +ve and CD105 +ve cells denoted a significant ($p<0.05$) decrease in subgroup S2 compared to subgroup S1 (Table 1).

Discussion

The current study demonstrated ameliorating effect of cord blood HMSC therapy on ADR induced chemobrain in an experimental model of albino rat. ADR was proved to be a commonly used chemotherapeutic drug, as evidenced by Blazkova et al. (17). This was evidenced by histological, histochemical, immunohistochemical and morphometric methods.

In subgroup A1 (rats sacrificed two weeks following confirmation of brain damage) some fields showed multiple vacuoles in the superficial layer of the cerebral cortex and occasional vacuoles containing cellular debris. Some shrunken nerve cells exhibiting dark nuclei and surrounded by vacuoles existed. These results suggested induced degenerative changes. In agreement, anticancer drugs were recorded to adversely affect the self-renewal potential of neural progenitor cells and also chromatin remodeling (18). It was also mentioned that ADR treatment increases the susceptibility of brain mitochondria to oxidative stress, predisposing brain cells to degeneration and death (19). ADR can damage normal noncancerous cells that might contribute to chemotherapy-induced cognitive deficits when administered either alone or in combination with other agents (20). Cancertherapy-related cognitive impairment is known as chemobrain or chemo-fog (21).

In subgroup A2 (rats sacrificed four weeks following confirmation of brain damage), partial separation of the surface of the cerebral cortex from the underlying layers,

Table 1. Area of shrunken nerve cells exhibiting dark nuclei, area % of PB +ve cells and area % of CD105 +ve cells in different groups and subgroups

Groups & subgroups	Area of shrunken nerve cells exhibiting dark nuclei	Area % of PB +ve cells	Area % of CD105 +ve cells
Control group	-	-	-
Subgroup A1	1225.81±198.07	-	-
Subgroup A2	2329.88±308.03*	-	-
Subgroup S1	1016.81±198.11	6.56±0.28	9.01±0.81
Subgroup S2	925.61±109.32	2.95±0.26*	5.63±0.43*

*significant ($p<0.05$).

large vacuoles were observed in the superficial layers and multiple vacuoles containing cellular debris were detected in the deeper layers. Multiple shrunken neurons exhibiting dark nuclei and surrounded by vacuoles were seen. These changes indicated more marked degenerative changes that progressed in relation to duration, which was confirmed by a significant increase in the area% of shrunken nerve cells exhibiting dark nuclei.

In subgroup S1 (rats sacrificed two weeks following SC therapy), brain sections showed localized areas recruiting vacuoles, occasional distended and occasional congested vessels. Some shrunken nerve cells containing dark nuclei and surrounded by minimal vacuoles were seen. The previous results indicated regression of morphological changes. It could be also commented that these reflex vascular changes help attraction and migration of injected therapeutic SCs to the site of injury. In agreement, it was indicated that intrathecal administration of MSCs by lumber puncture may be useful for treatment of brain injuries, such as stroke, or neurodegenerative disorders (22). Another study confirmed distinct effects on the metabolic viability and neuronal cell densities in primary cultures by administration of MSCs (23). A recent study proved that cord blood MSCs have a neuroprotective effect in neonatal hypoxia-ischemia. The mechanisms of action appear to be including immunomodulation, activation of endogenous stem cells, release of growth factors, and anti-apoptotic effects (24). High proliferative rate, non-invasive extraction and neural predisposition, is a powerful argument for the use of the intact isolated MSCs as a substrate in cell therapy to repair nerve tissue (25).

In subgroup S2 (rats sacrificed four weeks following SC therapy), some shrunken nerve cells with dark nuclei and surrounded by minimal vacuoles were found. However multiple normal pyramidal nerve cells were also noted. This denoted duration dependant regression of degenerative changes proved morphometrically.

The area% of Pb +ve and CD105 +ve cells denoted a significant decrease in subgroup S2 compared to subgroup S1, indicating differentiation of MSCs into repaired nerve cells.

It could be concluded that adriamycin induced progressive duration dependant cerebral degenerative changes. The morphological findings were confirmed by morphometric assessment. Cord blood human mesenchymal stem cell therapy proved definite amelioration of the degenerative changes. A reciprocal relation was recorded between the extent of regeneration and the existance of undifferentiated mesenchymal stem cells.

Potential conflict of interest

The authors have no conflicting financial interest.

References

1. Scherling CS, Smith A. Opening up the window into "chemobrain": a neuroimaging review. Sensors (Basel) 2013;13: 3169-3203
2. Lu RM, Chen MS, Chang DK, Chiu CY, Lin WC, Yan SL, Wang YP, Kuo YS, Yeh CY, Lo A, Wu HC. Targeted drug delivery systems mediated by a novel Peptide in breast cancer therapy and imaging. PLoS One 2013;8:e66128
3. Van Calsteren K, Hartmann D, Van Aerschot L, Verbesselt R, Van Bree R, D'Hooge R, Amant F. Vinblastine and doxorubicin administration to pregnant mice affects brain development and behaviour in the offspring. Neurotoxicology 2009;30:647-657
4. Yan M, Sun M, Zhou Y, Wang W, He Z, Tang D, Lu S, Wang X, Li S, Wang W, Li H. Conversion of human umbilical cord mesenchymal stem cells in Wharton's jelly to dopamine neurons mediated by the Lmx1a and neurturin in vitro: potential therapeutic application for Parkinson's disease in a rhesus monkey model. PLoS One 2013;8:e64000
5. Lee VW, Qin X, Wang Y, Zheng G, Wang Y, Wang Y, Ince J, Tan TK, Kairaitis LK, Alexander SI, Harris DC. The CD40-CD154 co-stimulation pathway mediates innate immune injury in adriamycin nephrosis. Nephrol Dial Transplant 2010;25:717-730
6. Zhu J, Zhang J, Xiang D, Zhang Z, Zhang L, Wu M, Zhu S, Zhang R, Han W. Recombinant human interleukin-1 receptor antagonist protects mice against acute doxorubicin-induced cardiotoxicity. Eur J Pharmacol 2010;643:247-253
7. Zickri M, Refaat N, Abdl Wahab N. Histological and immunohistochemical study on the effect of alpha-tocopherol (vitamin E) on doxorubicin (adriamycin) induced nephrotoxicity in albino rat. The 27th Scientific Conference of the Egyptian Society of Histology and Cytology 2003.
8. Lee YG, Hwang JW, Park SB, Shin IS, Kang SK, Seo KW, Lee YS, Kang KS. Reduction of liver fibrosis by xenogeneic human umbilical cord blood and adipose tissue-derived multipotent stem cells without treatment of an immunosuppressant. TERM 2008;5:613-621
9. Stocum DL, Zupanc GK. Stretching the limits: stem cells in regeneration science. Dev Dyn 2008;237:3648-3671
10. Koch TG, Heerkens T, Thomsen PD, Betts DH. Isolation of mesenchymal stem cells from equine umbilical cord blood. BMC Biotechnol 2007;7:26
11. Kraitchman DL, Heldman AW, Atalar E, Amado LC, Martin BJ, Pittenger MF, Hare JM, Bulte JW. *In vivo* magnetic resonance imaging of mesenchymal stem cells in myocardial infarction. Circulation 2003;107:2290-2293
12. Haasters F, Prall WC, Anz D, Bourquin C, Pautke C, Endres S, Mutschler W, Docheva D, Schieker M. Morphological and immunocytochemical characteristics indicate the yield of early progenitors and represent a quality control for human mesenchymal stem cell culturing. J Anat 2009;

214:759-767
13. Kiernan JA. Histological and Histochemical methods: theory and practice. 3rd ed. London, New York & New Delhi: Arnold Publisher; 2001. 111-162
14. Ellis R. Perls Prussian blue Stain Protocol, Pathology Division, Queen Elizabeth Hospital: South Australia 2007
15. Yagi H, Soto-Gutierrez A, Navarro-Alvarez N, Nahmias Y, Goldwasser Y, Kitagawa Y, Tilles AW, Tompkins RG, Parekkadan B, Yarmush ML. Reactive bone marrow stromal cells attenuate systemic inflammation via sTNFR1. Mol Ther 2010;18:1857-1864
16. Emsley R, Dunn G, White IR. Mediation and moderation of treatment effects in randomised controlled trials of complex interventions. Stat Methods Med Res 2010;19:237-270
17. Blazkova I, Nguyen HV, Dostalova S, Kopel P, Stanisavljevic M, Vaculovicova M, Stiborova M, Eckschlager T, Kizek R, Adam V. Apoferritin modified magnetic particles as Doxorubicin carriers for anticancer drug delivery. Int J Mol Sci 2013;14:13391-13402
18. Briones TL, Woods J. Chemotherapy-induced cognitive impairment is associated with decreases in cell proliferation and histone modifications. BMC Neurosci 2011;12:124
19. Cardoso S, Santos RX, Carvalho C, Correia S, Pereira GC, Pereira SS, Oliveira PJ, Santos MS, Proença T, Moreira PI. Doxorubicin increases the susceptibility of brain mitochondria to Ca^{2+}-induced permeability transition and oxidative damage. Free Radic Biol Med 2008;45:1395-1402
20. Aluise CD, Sultana R, Tangpong J, Vore M, St Clair D, Moscow JA, Butterfield DA. Chemo brain (chemo fog) as a potential side effect of doxorubicin administration: role of cytokine-induced, oxidative/nitrosative stress in cognitive dysfunction. Adv Exp Med Biol 2010;678:147-156
21. Mandilaras V, Wan-Chow-Wah D, Monette J, Gaba F, Monette M, Alfonso L. The impact of cancer therapy on cognition in the elderly. Front Pharmacol 2013;4:48-51
22. Lim JY, Jeong CH, Jun JA, Kim SM, Ryu CH, Hou Y, Oh W, Chang JW, Jeun SS. Therapeutic effects of human umbilical cord blood-derived mesenchymal stem cells after intrathecal administration by lumbar puncture in a rat model of cerebral ischemia. Stem Cell Res Ther 2011;2:38
23. Ribeiro CA, Fraga JS, Grãos M, Neves NM, Reis RL, Gimble JM, Sousa N, Salgado AJ. The secretome of stem cells isolated from the adipose tissue and Wharton jelly acts differently on central nervous system derived cell populations. Stem Cell Res Ther 2012;3:18
24. Phillips AW, Johnston MV, Fatemi A. The potential for cell-based therapy in perinatal brain injuries. Transl Stroke Res 2013;4:137-148
25. Zemel'ko VI, Kozhukharova IB, Alekseenko LL, Domnina AP, Reshetnikova GF, Puzanov MV, Dmitrieva RI, Grinchuk TM, Nikol'skiĭ NN, Anisimov SV. Neurogenic potential of human mesenchymal stem cells isolated from bone marrow, adipose tissue and endometrium: a comparative study. Tsitologiia 2013;55:101-110